Electrical Properties of Diamond Surfaces Functionalized with Molecular Monolayers†

Kiu-Yuen Tse‡, Beth M. Nichols‡, Wensha Yang‡, James E. Butler,§ John N. Russell, Jr.,§ and Robert J. Hamers*,‡

Department of Chemistry, University of Wisconsin−Madison, 1101 University Avenue, Madison, Wisconsin 53706, and Chemistry Division, Naval Research Laboratory, 4555 Overlook Avenue Southwest, Washington, D.C. 20375

Received: August 9, 2004; In Final Form: January 19, 2005

Recent studies have shown that semiconductor surfaces such as silicon and diamond can be functionalized with organic monolayers, and that these monolayer films can be used to tether biomolecules such as DNA to the surfaces. Electrical measurements of these interfaces show a change in response to DNA hybridization and other biological binding processes, but the fundamental nature of the electrical signal transduction has remained unclear. We have explored the electrical impedance of polycrystalline and single-crystal diamond surfaces modified with an organic monolayer produced by photochemical reaction of diamond with 1-dodecene. Our results show that, by measuring the impedance as a function of frequency and potential, it is possible to dissect the complex interfacial structure into frequency ranges where the total impedance is controlled by the molecular monolayer, by the diamond space-charge region, and by the electrolyte. The results have implications for understanding the ability to use molecularly modified semiconductor surfaces for applications such as chemical and biological sensing.

1. Introduction

Surfaces modified with organic monolayers have interesting physical and electrical properties that can be utilized for a variety of technological applications. In particular, monolayers also provide a pathway for subsequent functionalization of the surfaces with molecules for applications such as biological sensing.[1−4] A great deal of attention has been paid to self-assembled monolayers (SAMs) on gold[5−8] and, recently, molecular monolayers on silicon.[2,4,9−18] However, much less is known about monolayers on diamond.[1,19,20] The potential importance of molecular layers on diamond is highlighted by recent studies showing that when diamond thin films are covalently linked to biomolecules such as DNA, the resulting adducts have outstanding chemical stability.[1,21] Furthermore, electrical measurements show that the resulting surfaces can be used to achieve direct electronic sensing of biological binding events.[20,22,23]

To understand the basic physical processes that underlie the potential use of molecularly functionalized surfaces of diamond and other semiconductors as a basis for chemical or biological sensing elements, it is necessary to understand the electrical properties of the monolayer films. Previous studies have shown that the electrical properties of clean and hydrogen-terminated diamond are complicated by the polycrystalline nature of the films typically used[24−27] and by the fact that hydrogen diffusion into the bulk produces inhomogeneous doping distributions.[28] While these factors lead to nonideal behavior, the outstanding chemical stability[1,21] and emerging use of biomolecular interfaces to diamond for electronic biosensing[20,22,23] motivates a desire to understand the electrical properties of molecular layers on diamond. Here, we report investigations of the electrical properties of organic monolayers formed on polycrystalline diamond surfaces, and compare these with monolayers on single-crystal diamond and single-crystal silicon samples.

2. Experimental Methods

2.1. Substrates. The polycrystalline diamond films used are boron-doped (p-type) polycrystalline diamond thin films approximately 1.5 μm thick, grown on conductive p-type Si(110) substrate (500 μm thick, resistivity <0.005 Ω cm) at the Naval Research Laboratory. P-type doping was achieved by introducing 2 sccm B_2H_6 into the gas mixture during growth, which is expected to yield a dopant concentration of approximately 10^{19} cm^{-3}. Additional experiments were performed on a large type IIb natural diamond cleavage face, which was shown to have an average orientation 1° off the (111) surface. Silicon samples were lightly doped p-type (111) wafers with a specified resistivity of 12−18 Ω cm.

2.2. Photochemical Functionalization. Previous studies have shown that hydrogen-terminated surfaces of silicon[2,10,15] and diamond[1,3,19,20] can both be modified by a similar procedure, as depicted in Figure 1. To produce H-terminated diamond surfaces, the diamond films were cleaned in a series of acid baths and then terminated with hydrogen by heating the sample to 500 °C in a 13.56 MHz inductively coupled hydrogen plasma (20 Torr) for 5 min and then cooling to room temperature before extinguishing the plasma. The silicon samples were hydrogen-terminated by immersing them into nitrogen-purged 40% NH_4F solution and then rinsing with N_2-purged deionized water.[29] H-terminated diamond and H-terminated silicon samples were then functionalized by placing a small drop of 1-dodecene onto the sample, directly covering the thin fluid film with a quartz cover slip, and illuminating through the cover slip with ultraviolet light from a low-pressure mercury lamp (254 nm, 0.35 mW/cm^2) under an atmosphere of dry nitrogen. The

† Part of the special issue "George W. Flynn Festschrift".

* To whom correspondence should be addressed. Phone: (608) 262-6371. Fax: (608) 262-0453. E-mail: rjhamers@facstaff.wisc.edu.

‡ University of Wisconsin−Madison.

§ Naval Research Laboratory.

10.1021/jp046433w CCC: $30.25
Published on Web 03/05/2005

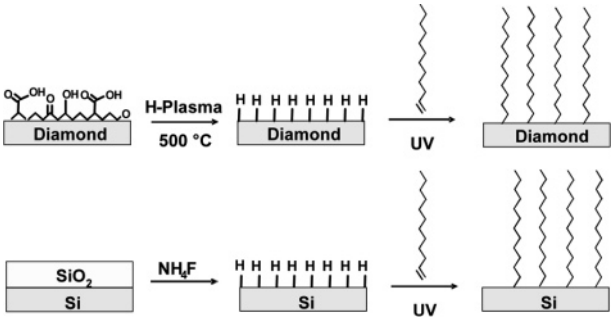

Figure 1. Schematic illustration of the procedure used to modify the diamond and silicon surfaces with an organic monolayer.

reaction times used were 12 h for diamond and 2 h for silicon, on the basis of previous measurements which showed that these reaction times produce self-terminating molecular monolayers.[2,15,19,30]

2.3. X-ray Photoelectron Spectroscopy. X-ray photoelectron spectroscopy (XPS) was used to optimize the conditions for H-termination, to determine the amount of oxygen on the surface, and to quantitatively determine the extent of functionalization of molecular layers on diamond surfaces. XPS measurements were performed using a Physical Electronics system with a monochromatized Al Kα source and a hemispherical analyzer with a 16-channel detector array.

2.4. Electrical Characterization. Electrical properties were characterized using impedance spectroscopy in a three-electrode electrochemical flow cell. In this cell, the chemically functionalized surface (H-terminated or dodecene-modified) was used as the working electrode and Pt foil as the counter electrode. A Viton O-ring was pressed against the working electrode to give an exposed geometric area of 0.08 cm^2. The two planar electrodes were separated by a thin sheet of poly(dimethylsiloxane) (PDMS), forming a fluid cell containing an embedded Ag/AgCl reference electrode. Ohmic contact was made to the rear side of the sample using a gallium indium eutectic. The experiments were performed at room temperature in 0.1 or 1 M aqueous KCl solution as stated. The solution was purged continuously with nitrogen during the experiment, and was pumped through the cell at a rate of 0.1 mL/min using a syringe pump. Impedance spectra were measured using a three-electrode potentiostat (Solartron 1287) and impedance analyzer (Solartron 1260) with Zplot software (Scribner Associates, Inc). All electrochemical potentials discussed below are with respect to the Ag/AgCl reference electrode.

3. Results

3.1. Cleaning and Functionalization. Figure 2 shows XPS measurements of a diamond thin film before and after plasma treatment. In the C(1s) region (Figure 2a), the oxidized surface shows several small C(1s) peaks at ~284.9 and 286.0 eV arising from various oxidized forms of carbon, in addition to the large peak at 284.5 eV. After H-plasma treatment, the C(1s) spectrum exhibits a single, sharp peak at 284.5 eV. The O(1s) region (Figure 2b) of the oxidized surface shows a large peak at 532.4 eV and a slightly smaller peak at 533.7 eV. After H-plasma treatment, the O(1s) region shows only a very small peak near 532.4 eV. Quantitative measurements give an O(1s)/C(1s) peak area ratio of 0.15 and 0.023 for the oxidized and plasma-treated samples; correction for the atomic sensitivity factors gives a value of the O/C ratio within the sampling depth of 0.062 for the oxidized surface, which is reduced to 0.009 after H-plasma treatment. Correcting for the inelastic mean free path and density

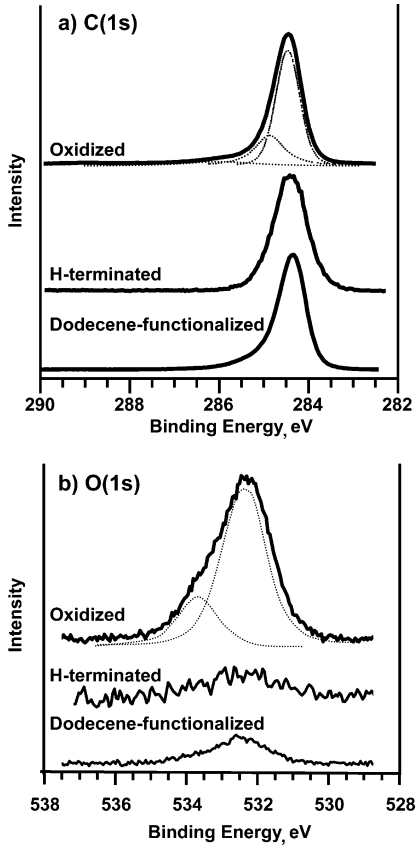

Figure 2. XPS data of oxidized, H-terminated, and dodecene-modified polycrystalline diamond surfaces: (a) C(1s) spectra, including a fit of the oxidized diamond spectrum to two peaks; (b) O(1s) spectra, including a fit of the oxidized diamond spectrum to two peaks.

of diamond yields a total of <0.1 monolayer (oxygen atoms per carbon atom in the surface layer) on the H-terminated surface. Single-crystal diamonds typically yield even lower amounts of residual oxygen than polycrystalline samples; this suggests that the small remaining oxygen that is detected on polycrystalline films likely arises from grain-boundary regions that are not accessible to the hydrogen plasma but are within the electron escape depth detected by XPS. Nevertheless, our XPS data show that the H-plasma treatment is effective at removing almost all surface oxygen from both polycrystalline and single-crystal samples.

Figure 2 also shows XPS spectra obtained after a H-terminated sample was functionalized with dodecene as described above. Functionalization with dodecene leads to the formation of a small tail on the high-binding-energy side of the main C(1s) peak. There is no detectable change in the O(1s) spectrum, indicating that the photochemical modification does not induce any detectable additional oxidation.

Additional experiments using similar molecules bearing fluorine or nitrogen-bearing species on polycrystalline diamond,[1,19] single-crystal diamond,[30] and single-crystal silicon[14] show that the molecular density of layers produced by the photochemical bonding is similar to that of layers produced by self-assembled monolayers on gold. These experiments lead to the conclusion that although the molecular monolayers on diamond and silicon do not have long-range order, the molecules are closely packed, limited by the physical dimensions of the alkyl chains.

3.2. Electrical Characterization of Dodecene-Modified Polycrystalline Diamond Film. Figure 3 shows impedance spectra of a dodecene-modified polycrystalline diamond surface

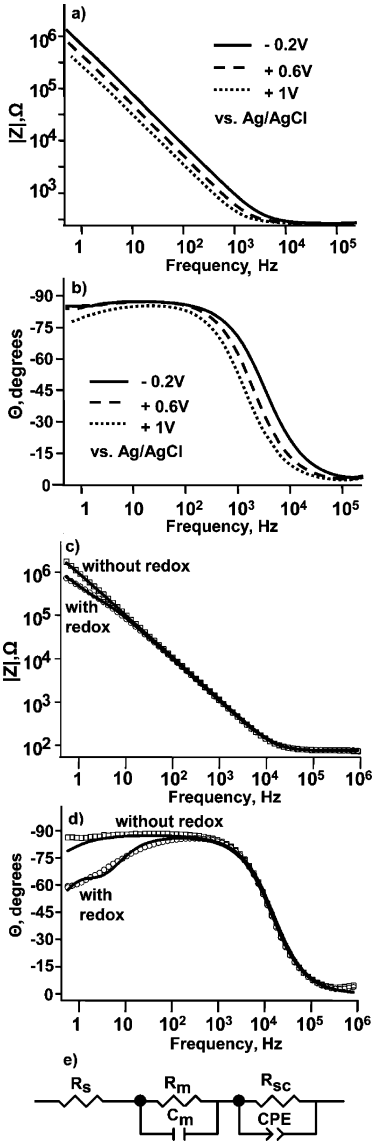

Figure 3. (a) Absolute impedance of dodecene-modified diamond as a function of frequency at different potentials. (b) Phase angle as a function of frequency at different potentials. (c) Magnitude of impedance in the presence and absence of redox agent. Markers show experimental data, and the line shows a fit to a circuit model. (d) Phase angle in the presence and absence of redox agent. Markers show data, and the line shows a fit to a circuit model. (e) Circuit model used in fitting the data for (c) and (d).

in a 0.1 M KCl solution, measured at three different dc potentials. In impedance spectroscopy, the potential of the sample is modulated by a small sinusoidal excitation signal (typically 10 mV root-mean-square), and the in-phase and out-of-phase components of the current at the modulation frequency f are measured.[31] Measuring the in-phase and out-of-phase components of the current as the modulation frequency f is swept over a wide range (here, 0.5 Hz to 1 MHz) yields a frequency spectrum of the electrical response. Because the current and voltage do not necessarily have the same phase and are frequency-dependent, the impedance Z is usually described as a complex, frequency-dependent quantity. The complex impedance is defined as $\hat{Z} = \hat{V}/\hat{I} = Z' + iZ''$. The data are usually presented as plots of the magnitude ($|Z|$) and phase angle (θ) of the impedance as a function of frequency f; alternatively, the data can be represented in complex form as the real part (Z') and the imaginary part (Z'') of the impedance as a function of frequency f.

The three impedance spectra in Figure 3a all show similar behavior. At the lowest frequencies measured the total impedance is very high, in excess of 1 MΩ. As the frequency increases the impedance decreases linearly with frequency, while the phase angle θ (Figure 3b) is close to $-90°$ ($-87°$ at $f = 1$ Hz) up to a frequency of ~1 kHz. Since an ideal capacitor has a $\theta = -90°$, this result indicates that at very low frequencies the interface behaves very nearly like an ideal capacitor. At the very lowest frequencies the phase angle deviates slightly from $-90°$; we attribute this deviation to the presence of a small number of conductive defects in the monolayer, giving rise to a large but finite molecular resistance in parallel with the molecular capacitance. Above ~1 kHz, the impedance reaches a limiting value and θ approaches 0° ($-2.7°$ at $f = 500$ kHz); in this region the impedance is limited by the uncompensated solution resistance. Because the solution resistance is determined in part by the physical separation between the sample and the reference electrode, the apparent transition from capacitive to resistive behavior (here, ~10 kHz) is dependent on the cell geometry; moving the reference electrode closer to the sample decreases the solution resistance and extends the capacitive region out to higher frequencies. The origin of the small departure from perfect resistive behavior (minimum phase angle of $-2.7°$ instead of 0°) is unclear, but likely arises from the finite response time of the Ag/AgCl electrode and small phase shifts within the instrumentation. Overall, the data show that dodecene-modified diamond surfaces in KCl are capacitive at low frequencies and resistive at high frequencies, with only small deviations from ideal behavior.

In addition to the strong frequency dependence, Figure 3a also shows that the impedance of the dodecene-modified diamond sample is dependent on the dc potential. At the most positive potential (+1.0 V) and lowest frequencies, the phase angle shifts away from $-90°$ and toward zero as the frequency is decreased; this behavior arises because at +1.0 V electrochemical oxidation of the diamond and/or the dodecene layer occurs, giving rise to a resistive element in parallel with the molecular capacitance. More significantly, at all frequencies <~1 kHz, where the impedance behaves capacitively, the impedance decreases as the dc potential is increased from -0.2 V to more positive values.

The potential dependence observed in Figure 3 is typical for a p-type semiconductor in which there is a subsurface depletion region. At semiconductor surfaces, exchange of charge with surface defects or into the solution often shifts the energies of the conduction and valence bands such that, at the surface, the Fermi level lies approximately midway between valence and conduction bands. This mid-gap Fermi level position is accompanied by formation of a subsurface depletion region (also referred to as the space-charge region) in which the semiconductor is largely depleted of mobile charge carriers, resulting in a high impedance. For a p-type semiconductor, the depletion region is reduced as the potential is made more positive. At the "flat-band potential" V_{fb} the depletion zone is eliminated, and at more positive potentials an accumulation layer is formed with a very high density of holes, and a very high conductivity. In Figure 3, the ability of an external applied field to induce a significant change in the space-charge layer demonstrates that the density of midgap surface states is small enough to avoid "pinning" of the Fermi energy by these surface states.

The electric field effect in Figure 3a,b is critical for the utility of molecular monolayers as insulating films for field-effect molecular or biomolecular sensing devices.[4,20,22,23] Since in these devices oxidation−reduction currents are undesirable, most of

TABLE 1: Results of Fitting the Data in Figure 3c,d to the Circuit Model Shown in Figure 3e[a]

	R_s,Ω	R_m, Ω	C_m, F	R_{sc},Ω	CPE-T	CPE-P
with redox	66	85000	4.4×10^{-7}	1.8×10^{6}	4.6×10^{-7}	0.94
without redox	66	∞ ($>10^{20}$)	3.6×10^{-7}	1.8×10^{6}	4.6×10^{-7}	0.94

[a] The data have not been corrected for the sample area of 0.08 cm^2.

our measurements were performed using KCl solutions with no added oxidation−reduction couple. However, parts c and d of Figure 3 show how the presence of a redox agent affects the measured electrical properties. The data points represented by open markers show the amplitude and phase of the impedance of a dodecene-modified diamond sample in pure 1 M KCl, and for the same sample in a 1 M KCl solution containing 0.001 M $K_3Fe(CN)_6$ and 0.001 M $K_4Fe(CN)_6$. The presence of the redox agent decreases the impedance at low frequencies ($<\sim$10 Hz) and shifts its phase toward 0°. These effects are readily attributed to defects or other pinholes in the film that allow a small amount of penetration of ions through the molecular layer. The data in Figure 3c,d can be reasonably fit to a single equivalent circuit model (shown in Figure 3e) in which only the values of the molecular capacitance C_m and molecular resistance R_m change; these fits are represented by the lines in Figure 3c,d, and the actual component values are shown in Table 1. In this circuit model we have used a constant phase element (CPE).[31] The CPE has an impedance defined by

$$\hat{Z} = 1/T(i\omega)^P$$

where T is defined such that when $P = 1$, T is in units of farads. The CPE is a generalized capacitance that is sometimes employed to account for microscopic roughness; however, it has also been used on flat diamond surfaces to account for nonuniform distribution of dopants.[28] The value of P of $\sim$0.94 that we observe indicates that deviations from perfect capacitive behavior are small, and we find that using a capacitor instead of a CPE results in only a slight degradation in the quality of the fit. A comparison of the fits with three different equivalent circuit models can be found in the Supporting Information.

While the redox agent affects the apparent capacitance and resistance of the molecular layer, the effects are obvious only at low frequencies. At higher frequencies, the redox agent has no significant effect on the impedance measurements even though the instantaneous currents at high frequencies are larger.

To identify the influence of solution resistance on the impedance spectra, identical experiments were performed after the KCl concentration was increased from 0.1 to 1.0 M. Figure 4 shows impedance spectra of a dodecene-modified diamond sample in 0.1 and 1.0 M KCl solutions, biased at 0 V vs Ag/AgCl. Parts a and b of Figure 4 show the results as the magnitude and phase of the impedance, while Figure 4c shows the same data presented as the real (Z') and imaginary (Z'') parts of the complex impedance. From Figure 4a,b, it is clear that increasing the solution concentration has a significant effect on the absolute impedance only at very high frequency. Moreover, Figure 4c shows that these changes occur almost primarily in the real part (Z') of the impedance (Figure 4c), with very little effect on the imaginary part (Z'').

Figure 4d shows the effective capacitance, extracted from the data in Figure 4c using $C = -1/2\pi fZ''$. When the electrolyte concentration is increased from 0.1 to 1.0 M, Figure 4d shows that there is a small decrease of $\sim$20% in the total capacitance. This is in stark contrast to what would be expected from the electrical double layer. According to Gouy−Chapman theory, the capacitance per unit area of the electrical double layer is

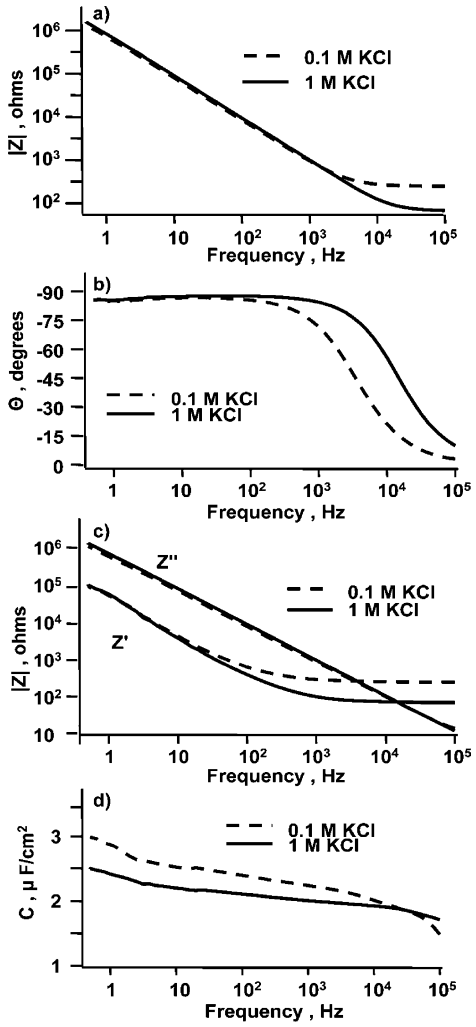

Figure 4. Impedance spectra of the monolayer-modified polycrystalline diamond film, in 0.1 and 1 M KCl solution as specified, biased at 0 V vs Ag/AgCl: (a) absolute impedance; (b) phase angle; (c) real and imaginary parts of the impedance; (d) capacitance.

given by $C_A = (2F^2M\epsilon\epsilon_0/RT)^{1/2}$, where F is the Faraday constant (96487 C/mol), M is the concentration of ions (mol/m^3), R is the universal gas constant (8.314 J mol^{-1} K^{-1}), T is temperature (K), ϵ_0 is the permittivity of free space, and ϵ is the dielectric constant.[32] In a 0.1 M KCl solution, this yields a capacitance of 73 μF/cm^2. This calculated double-layer capacitance is much larger than the value observed in our experiments. Furthermore, since the double-layer capacitance increases with the square root of the ionic concentration, if the measured capacitance were due to the double layer, we would expect the capacitance to increase by a factor of $\sim$3 when the KCl concentration is increased from 0.1 to 1.0 M. Since our measured capacitance values are much smaller than those predicted for the double layer and show only a weak dependence on ionic concentration, we conclude our measured capacitance values are not controlled by the electrolyte concentration, and that in general the electrolyte concentration does not significantly affect the measured impedance spectra except at the high frequencies where the interface behaves resistively and solution resistance becomes important.

The data in Figures 3 and 4 demonstrate several important facts. First, they show that the contribution of the resistance and capacitance of the solution to the total measured impedance can be separated from the contributions of the semiconductor and the molecular layer. Second, since the solution changes only

the real part of the impedance and leaves the imaginary part nearly unaffected, we conclude that the capacitance of the Helmholtz layer of the solution is large compared with the effective capacitance of the interface (i.e., the lumped capacitance of the diamond space-charge region and the molecular layer).[33] This is because the two capacitors are in series and the smaller space-charge capacitance will dominate the total capacitance. Finally, the data show that at frequencies >∼10 Hz the absolute impedance is controlled by the space-charge region of the diamond, but is not strongly affected by the presence of oxidation−reduction agents. Therefore, we conclude that at frequencies >∼10 Hz the impedance is controlled by the physical response of the materials (i.e., nonfaradic processes) rather than the rate of electron transfer (i.e., faradic processes) between the electrode and redox species in solution.

3.3. Mott−Schottky Plots of a Dodecene-Modified Polycrystalline Diamond Film. To further confirm that the field effect observed is due to the diamond film, and to further characterize the electrical properties of the surfaces, Mott−Schottky plots were performed. In the Mott−Schottky analysis, the complex impedance is modeled as an equivalent circuit consisting of a series resistor and capacitor,[33−36] and the capacitance can be calculated from the imaginary part of the impedance: $C = -1/2\pi fZ''$. This simple circuit model is consistent with the data in Figure 3. When the frequency-dependent data are fit to discrete circuit models, the data at frequencies between ∼100 Hz and 100 kHz are nearly independent of the circuit model and are fit nearly as accurately with a single series resistor and capacitor as with more elaborate models. Alternatively, the effective space-charge capacitance can be extracted by fitting a complete frequency spectrum to a model, and extracting the space-charge capacitance from the fit parameters. Fits to circuit models in the absence and presence of a redox agent and Mott−Schottky plots obtained from circuit model fitting are given in the Supporting Information. Here, we take the more conventional approach of using a simple series *RC* circuit, since its validity is established by more detailed modeling. Qualitatively, in the Mott−Schottky analysis the inverse square of the capacitance, $1/C^2$, is plotted against the dc potential V; for doped semiconductors this yields a sigmoidal plot. Under biasing conditions where the semiconductor space-charge region is in depletion, the capacitance of the space-charge region can be represented analytically as

$$\frac{1}{C^2} = \left(\frac{2}{eN_A\epsilon_0\epsilon}\right)\left(\left|V - V_{fb}\right| - \frac{kT}{e}\right) \quad (1)$$

where e is the electronic charge, N_A is the dopant (acceptor) density, ϵ_0 is the permittivity of free space, ϵ is the relative permittivity (or dielectric constant, 5.5 for diamond), V is the applied potential, V_{fb} is the flat band potential, k is the Boltzmann constant, and T is the temperature. Since the term kT/e is 0.026 V at room temperature and insignificant compared to the error introduced by the extrapolation, it can often be ignored, and eq 1 simplifies to

$$\frac{1}{C^2} = \left(\frac{2}{eN_A\epsilon_0\epsilon}\right)|V - V_{fb}| \quad (2)$$

Equation 2 shows that when the surface potential V is equal to the flat-band potential V_{fb}, $1/C^2$ is zero (x-intercept). In addition, the acceptor density N_A can be determined from the slope:

$$N_A = -\left(\frac{2}{e\epsilon_0\epsilon}\right)\left(\frac{d(1/C^2)}{dV}\right)^{-1} \quad (3)$$

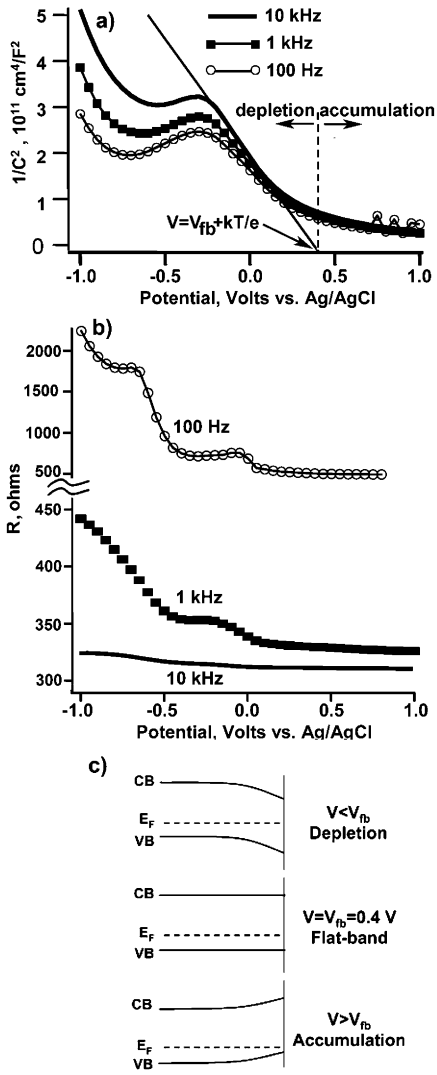

Figure 5. Potential-dependent measurements of the monolayer-modified polycrystalline diamond film in 0.1 M KCl solution, taken at different frequencies as specified: (a) Mott−Schottky plots; (b) resistance as a function of potential; (c) schematic illustration of band edges corresponding to depletion, flat-band, and accumulation regions.

Figure 5a shows the Mott−Schottky plots of the monolayer-modified diamond film measured at frequencies of 100 Hz, 1 kHz, and 10 kHz. As expected, a sigmoidal plot is observed, with an overall shape consistent with that expected for a p-type semiconductor. At potentials more negative than ∼−0.5 V reduction of H^+ to H_2 occurs, leading to anomalous behavior in the resistance and capacitance.

The slight frequency dispersion has several possible origins:[37] (1) dielectric relaxation in the space-charge region; (2) surface roughness of the electrode; (3) slow ionization of deep acceptor levels in the space charge region; (4) the effect of surface states. Quantitative analysis of the Mott−Schottky plot yields the dopant density and flat-band potential. Visual inspection of Figure 5 shows that the plots are linear between −0.25 and +0.2 V. Fitting the 10 kHz data to a straight line yields an acceptor density of 5×10^{19} cm^{-3}, on the basis of the projected macroscopic surface area of 0.08 cm^2. Use of the microscopic surface area by incorporating a surface roughness factor would yield a slightly lower acceptor density. While quantitative measurement of the conductivity of diamond films is very difficult because of depth-dependent variations in the effective

dopant concentration[28] and the presence of an underlying silicon substrate, the value obtained from our impedance measurements is in good agreement with the value expected for our growth conditions.[27] Extrapolation of the linear region to $1/C^2 = 0$ yields a flat-band potential of 0.4 V. Previous studies of H-terminated diamond have reported a broad range of values, from +0.4 to +1 V vs Ag/AgCl.[27,38] This broad range arises in large part because of variations in surface terminations, as diamond surfaces that are oxidized show more positive flat-band potentials.[39] The flat-band potential of 0.4 V that we observe is consistent with the expected termination of the surface by alkyl chains or remaining H atoms, and the almost complete absence of surface oxidation that is also revealed by the low O(1s) intensity in the XPS measurements of Figure 2.

The strong variation of capacitance with voltage also implies that when the dc potential is changed, most of the potential drop occurs within the diamond. This is also supported by Figure 5b, where the resistance is plotted as a function of potential. It is noteworthy that unterminated "dangling bond" defects at semiconductor surfaces typically have energies near the middle of the band gap. Such defects typically give rise to a pronounced peak in the resistance vs potential curve.[40] In contrast, in Figure 5b the plot varies smoothly with no evidence for a significant peak. This suggests that the dodecene-modified diamond interface is relatively free of charge-trapping defects.

3.4. Hydrogen-Terminated Polycrystalline Diamond Film. Electrical measurements were also performed on diamond surfaces immediately after hydrogen termination. Parts a and b of Figure 6 show impedance spectra of a H-terminated diamond surface in a 0.1 M KCl solution. The impedance spectra trace each other very well during the course of the electrical measurement, indicating that the surface remains hydrogen-terminated in the nitrogen-purged KCl solution. Comparison with Figure 3 reveals that the impedance spectra of H-terminated diamond are quite similar to those of the dodecene-modified surface. Mott−Schottky plots (Figure 6c) at frequencies of 100 Hz, 1 kHz, and 10 kHz all show the sigmoidal shape characteristic of the p-type semiconductor. A Mott−Schottky analysis of the 10 kHz data yields an acceptor density of 8×10^{19} cm^{-3} and a flat-band potential of 0.1 V (vs Ag/AgCl), both of which are similar to those measured for the dodecene-modified surface. The total interface capacitance obtained from Figure 6, approximately 2.5 μF/cm^2, is also in good agreement with a previous measurement of 3.4 μF/cm^2 on similar p-type diamond electrodes.[26] Figure 6d shows the real part of the impedance as a function of potential. Again, the structure is similar to that of the dodecene-modified surface, with no evidence for peaks associated with surface states.

3.5. Dodecene-Modified Single-Crystal Diamond. To investigate the impact of the surface roughness and grain boundaries on the field effect of the system, a piece of a naturally boron doped single-crystal diamond(111) sample was modified using the same procedures. Parts a and b of Figure 7 show impedance spectra (in 1 M KCl) of the single-crystal diamond that was modified with dodecene. The total impedance (at −0.2 V) on this sample is approximately 100 times larger than the values typically obtained on the polycrystalline diamond samples. The magnitude of the impedance changes significantly as a function of the applied potential, again decreasing as the potential is made more positive. Figure 7c shows the Mott−Schottky plots of the monolayer-modified single-crystal diamond, measured at 100 Hz, 1 kHz, and 10 kHz. The plots are qualitatively similar to those observed on polycrystalline thin films, except that there is a stronger dependence on frequency

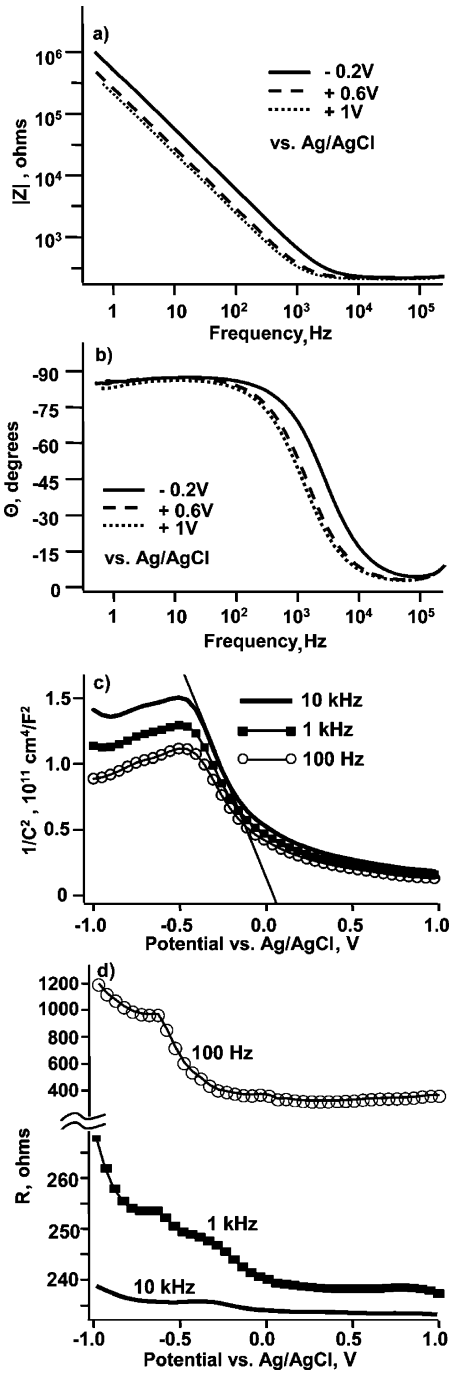

Figure 6. Electrical measurements of the hydrogen-terminated polycrystalline diamond film, in 0.1 M KCl solution: (a) absolute impedance as a function of frequency, biased at different potentials; (b) phase angle as a function of frequency, biased at different potentials; (c) Mott−Schottky plots at different frequencies; (d) resistance as a function of potential at different frequencies.

and a more complicated phase response. The flat-band potential of 0.8 V vs Ag/AgCl that is inferred from the 10 kHz data is slightly more positive than that observed on the highly doped thin film; this difference is due at least in part to the different Fermi level that accompanies the much lighter doping of the single crystal. From the linear part of the 10 kHz plot, an acceptor density of 9×10^{14} cm^{-3} is calculated. At negative potentials, the limiting value of $1/C^2$ yields a capacitance of 0.006 μF/cm^2. Compared with the polycrystalline samples, the dodecene-modified single-crystal diamond gives a dopant concentration 5 orders of magnitude lower and a limiting

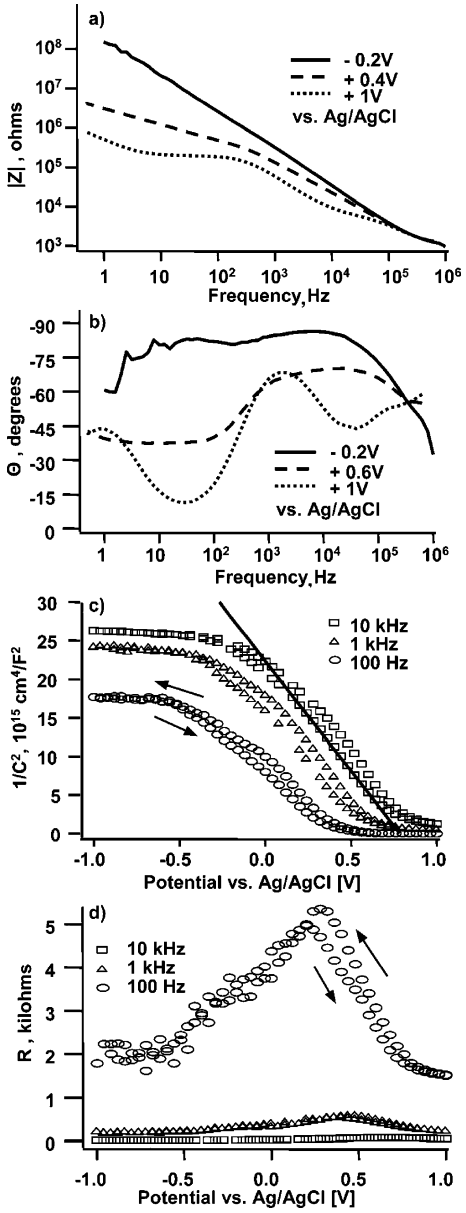

Figure 7. Electrical measurements of the dodecene-modified single-crystal diamond, in 1 M KCl solution: (a) absolute impedance as a function of frequency, biased at different potentials; (b) phase angle as a function of frequency, biased at different potentials; (c) Mott−Schottky plots at different frequencies; (d) resistance as a function of potential at different frequencies.

capacitance at negative potentials (depletion conditions) ~400 times smaller. Since

$$C_{SC} \propto \sqrt{N_A}$$

the differences in dopant concentration and capacitance are consistent with one another. On the single-crystal diamond sample, the resistance vs potential plot in Figure 7 shows a peak near +0.4 V, suggesting the presence of electronic states within the bulk band gap in the surface region.

3.6. Summary of Results from Diamond. The result sections above have shown that (1) the boron-doped polycrystalline diamond films, both organic-monolayer-modified and hydrogen-terminated, demonstrate a significant variation in impedance with applied potential and (2) the contributions of the solution electrolyte are important only at very high frequencies where the overall impedance behaves resistively and at very low frequencies (<~10 Hz). At most intermediate frequencies, the impedance is dominated by the diamond thin film, with some possible contribution from the dodecene layer.

3.7. Comparison with Dodecene-Modified Silicon. To provide a comparison of the field effect of the diamond samples with that of a well-studied semiconductor, similar measurements were made on dodecene-functionalized silicon surfaces. Polycrystalline diamond samples and single-crystal silicon samples with the same dopant concentration have very different conductivities because of the high activation energy of boron dopants in diamond (0.37 eV)[41] and because the grain boundaries of polycrystalline diamond scatter electrons, reducing the mobility of the charge carriers. Consequently, we chose to compare these under conditions where the total impedances were similar under open-circuit conditions. The polycrystalline diamond samples we used yield impedances that are comparable to those of silicon samples with resistivities on the order of 10 Ω cm.

Parts a and b of Figure 8 show impedance spectra of dodecene-modified p-type silicon wafers in 1 M KCl solution for several dc bias potentials. A comparison of these data with similar data on polycrystalline diamond (Figure 3a,b) shows that the silicon samples exhibit a more complex dependence on frequency and, in the 50 Hz to 5 kHz range, show a stronger influence of changing the applied potential. Figure 8c shows a Mott−Schottky plot of p-type silicon; this yields a flat-band potential of −0.37 V vs Ag/AgCl. The resistance (Figure 8d) shows a large peak near −0.53 V; a similar peak has been reported previously and attributed to electrically active surface states,[40] although there may be some contribution from hydrogen reduction.

4. Discussion

4.1. Comparison of Dodecene-Modified and H-Terminated Diamond. Our results show that the dodecene-modified and H-terminated diamond samples have many similar features. However, they exhibit different flat-band potentials, and the presence of the molecular layer contributes an additional capacitance to the systems. The shift in flat-band potential can be ascribed to a combination of two factors. First, since carbon is more electronegative (2.5) than hydrogen (2.1), the C−H bond of the H-terminated surface is polarized such that the carbon is slightly negative and hydrogen slightly positive; this would normally induce an upward band-bending, driving the surface toward accumulation and yielding a flat-band potential slightly negative of what would be expected for an ideal, nonpolar surface termination. Photochemical modification of dodecene therefore has the effect of making the bulk more positive, shifting the surface bands downward from those of the H-terminated surface. Perhaps more importantly, oxidation of the surface also is known to shift the bands downward, resulting in an even more positive flat-band potential. While our XPS measurements do not show any significant increase in surface oxygen after reaction with dodecene, this possibility cannot be excluded. Thus, the shift in flat-band potential is consistent with removal of hydrogen and the possibility of a small amount of oxidation.

We also note that the presence of the monolayer changes the interfacial capacitance. To extract the capacitance of the dodecene monolayer, we performed a more detailed analysis of the impedance spectra of samples before and after the photochemical modification step, to identify whether the molecular capacitance could be easily extracted from these data. The capacitance of the H-terminated and dodecene-modified

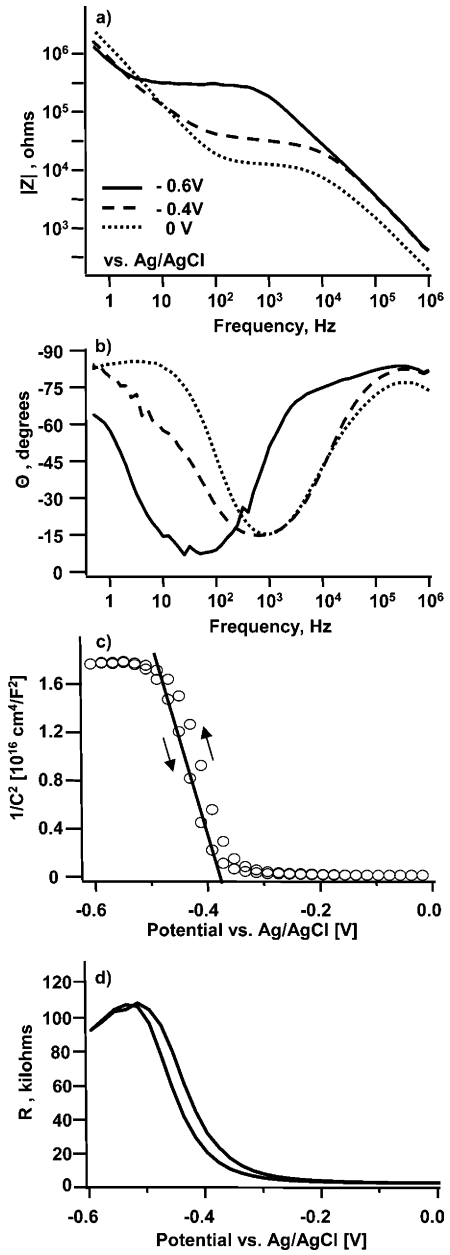

Figure 8. Impedance spectra of dodecene-modified p-type silicon, in 1 M KCl solution and biased at different potentials as specified: (a) magnitude of impedance; (b) phase angle; (c) Mott−Schottky plot at 10 kHz; (d) resistance at 10 kHz.

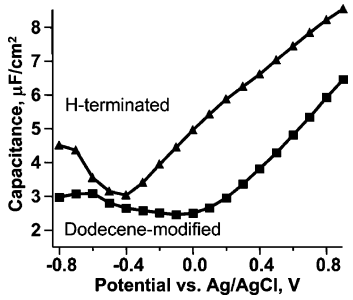

Figure 9. Capacitance vs potential of H-terminated and dodecene-modified polycrystalline samples.

samples were extracted by fitting the impedance spectra with a series RC Model. Figure 9 shows the total capacitance per unit area as a function of potential for H-terminated and dodecene-terminated samples. As the potential is changed, both samples show an apparent minimum in total capacitance; this minimum corresponds to 3.04 μF/cm^2 for the H-terminated sample (at a potential of −0.4 V) and 2.45 μF/cm^2 after functionalization (at −0.1 V). Assuming that the molecular layer shows a simple series capacitance, the effective molecular capacitance can then be calculated as ∼12.6 μF/cm^2. This value represents the total difference in capacitance of the two samples, and represents a lumped capacitance including the effects of the molecular layer as well as any new interface states that might be generated by the photochemical modification. This value is somewhat higher than the values previously reported for similar molecules on gold (∼1.5 μF/cm^2)[7,8] and on silicon (2.3 μF/cm^2).[13] The theoretical molecular capacitance per unit area can be estimated using

$$C_m = \frac{\epsilon_0 \epsilon}{d} \tag{4}$$

where ϵ_0 is the permittivity of free space, ϵ is the dielectric constant of the organic monolayer, and d is the thickness of the monolayer. Previous studies have reported molecular dielectric constants of 3.3 for an *n*-alkyl monolayer on silicon[13] and 2.6 for alkanethiols on gold,[7] compared with the value of 2.3 for polyethylene.[42] Using a value of 16 Å for the thickness of the monolayer (assuming the molecules extend fully normal to the surface)[7] yields a predicted value of ∼1.8 μF/cm^2 for the monolayer capacitance. Again, the value we observe is higher than expected.

We attribute the relatively high value of capacitance that we observe to three possible factors: (1) due to surface roughness the actual sample area is larger than the simple geometric area, (2) the actual dielectric constant is probably larger than the value of 3.3 used here because of penetration by water and ions into the molecular layer, and (3) the effective thickness of the monolayer is likely smaller than the value used, particularly if the molecules are not closely packed and hence do not extend fully or are tilted at an angle.

4.2. Comparison of Functionalized Diamond and Silicon Surfaces. The principal motivation for investigating diamond thin films is the possible use of molecularly modified diamond thin films as chemical or biological sensing elements. By linking specific molecular or biomolecular recognition elements at the surface, the binding of other charged species to the surface can be detected via the field effect, in which the charged molecules induce a band-bending in the semiconductor. [4,20,22,23,43,44] The fabrication of chemically and biologically sensitive field-effect devices has been significantly hampered by the fact that silicon and most other semiconductors are not stable in aqueous environments.[2,15] In contrast, diamond thin films that have been modified with biological molecules are extremely stable.[1,21]

Because silicon remains the most widely used semiconductor material, a comparison of functionalized diamond and functionalized silicon surfaces is warranted. Our Mott−Schottky data show that diamond surfaces are relatively free of charge-trapping defects, and that over a substantial part of the frequency range the impedance is dominated by the diamond space-charge layer, exhibiting a significant "field effect" in response to an external potential. However, the variation in impedance due to a given change in potential is somewhat larger on silicon than on polycrystalline diamond with similar total conductivity. We believe this difference arises in large part due to the relatively low mobilities in polycrystalline diamond thin films. The conductivity of a p-type semiconductor is controlled by the number of acceptors (N_A) and the hole mobility (μ_h). While it is possible to achieve hole mobilities in excess of 1300 cm^2

V^{-1} s^{-1} for single-crystal diamond[45] compared with ~450 cm^2 V^{-1} s^{-1} for silicon, in polycrystalline samples the electron scattering greatly reduces the mobility. Polycrystalline diamond samples typically have mobilities on the order of 0.5−10.0 cm^2 V^{-1} s^{-1},[41,46] anywhere from 100 to 1000 times smaller than the maximum values possible.

The low mobility of the charge carriers has an adverse effect on the ability to use diamond thin films as the basis for chemical or biological sensing because it reduces the change in current across the interface produced by a given change in potential at the surface. Molecular or biomolecular species binding to the surface change the charge distribution at the surface and thereby affect the energies of the valence and conduction bands; the resulting current flow depends not only on the band positions, but also on the mobility of the charge carriers. Consequently, the change in current resulting from binding of molecules to the functionalized interface is reduced if the mobility is low.

5. Conclusions

Our results show that organic (dodecene)-monolayer-modified boron-doped (single and polycrystalline) diamond surfaces show a significant field effect, whose direction is typical of a p-type semiconductor. The combination of frequency- and potential-dependent measurements provides a way to separate the properties of the electrolyte, the molecular layer, and the underlying semiconducting substrate.

Using molecular layers as an interface between semiconducting substrates and biological molecules in solution, it is possible to use the changes in potential associated with charged molecules to induce changes in conductivity in the subsurface space-charge region of the semiconductor.[4,20] The molecular layer plays several roles including (1) providing a covalent link to tether various biomolecular recognition agents such as DNA or other biomolecules to the surface, (2) reducing nonspecific binding of proteins and other molecules directly to the surface,[47] (3) helping to chemically stabilize the interface against unwanted chemical reactions, and (4) providing a well-defined electrically insulating layer between the semiconductor and the aqueous solution to block the flow of dc current. Balancing these roles involves a complex interplay between materials properties and chemistry.

Our experiments show that diamond thin films that have been modified with molecular monolayers exhibit many of the properties expected for a p-type semiconductor. In particular, the field effect, in which an external potential induces an electric field that penetrates into the subsurface region of the diamond, altering its conductivity. While our previous work shows that polycrystalline diamond surfaces have extremely good chemical stability, the current experiments show that these chemical properties are tempered by the fact that the polycrystalline nature of diamond thin films lowers the mobility of the charge carriers, which manifests itself in increased impedance of the film for comparable concentrations of electrically active dopants. To achieve moderate levels of conductivity requires high dopant concentrations, but these high concentrations reduce the mobility and reduce the influence of external potentials on the current. Thus, we conclude that the use of polycrystalline diamond thin films represents a tradeoff between improved chemical stability and sensitivity.

Acknowledgment. We acknowledge useful discussions and interactions with Dr. John Peck and Professor Dan van der Weide. This work was supported in part by National Science Foundation Grants CHE-0314618 and BES-0330257.

Supporting Information Available: Fits of the data from Figure 3c,d to three different circuit models of varying complexity and Mott−Schottky analysis of H-terminated and dodecene-modified diamond obtained by fitting of complete frequency spectra to a circuit model and extracting the space-charge capacitance as a function of potential (PDF). This material is available free of charge via the Internet at http://pubs.acs.org.

References and Notes

(1) Yang, W. S.; Auciello, O.; Butler, J. E.; Cai, W.; Carlisle, J. A.; Gerbi, J.; Gruen, D. M.; Knickerbocker, T.; Lasseter, T. L.; Russell, J. N.; Smith, L. M.; Hamers, R. J. *Nat. Mater.* **2002**, *1*, 253.

(2) Strother, T.; Cai, W.; Zhao, X. S.; Hamers, R. J.; Smith, L. M. *J. Am. Chem. Soc.* **2000**, *122*, 1205.

(3) Knickerbocker, T.; Strother, T.; Schwartz, M. P.; Russell, J. N.; Butler, J.; Smith, L. M.; Hamers, R. J. *Langmuir* **2003**, *19*, 1938.

(4) Cai, W.; Peck, J. R.; van der Weide, D. W.; Hamers, R. J. *Biosens. Bioelectron.* **2004**, *19*, 1013.

(5) Nuzzo, R. G.; Dubois, L. H.; Allara, D. L. *J. Am. Chem. Soc.* **1990**, *112*, 558.

(6) Bain, C. D.; Troughton, E. B.; Tao, Y. T.; Evall, J.; Whitesides, G. M.; Nuzzo, R. G. *J. Am. Chem. Soc.* **1989**, *111*, 321.

(7) Porter, M. D.; Bright, T. B.; Allara, D. L.; Chidsey, C. E. D. *J. Am. Chem. Soc.* **1987**, *109*, 3559.

(8) Boubour, E.; Lennox, R. B. *J. Phys. Chem. B* **2000**, *104*, 9004.

(9) Barrelet, C. J.; Robinson, D. B.; Cheng, J.; Hunt, T. P.; Quate, C. F.; Chidsey, C. E. D. *Langmuir* **2001**, *17*, 3460.

(10) Cicero, R. L.; Linford, M. R.; Chidsey, C. E. D. *Langmuir* **2000**, *16*, 5688.

(11) Linford, M. R.; Chidsey, C. E. D. *J. Am. Chem. Soc.* **1993**, *115*, 12631.

(12) Linford, M. R.; Fenter, P.; Eisenberger, P. M.; Chidsey, C. E. D. *J. Am. Chem. Soc.* **1995**, *117*, 3145.

(13) Yu, H. Z.; Morin, S.; Wayner, D. D. M.; Allongue, P.; de Villeneuve, C. H. *J. Phys. Chem. B* **2000**, *104*, 11157.

(14) Lin, Z.; Strother, T.; Cai, W.; Cao, X.; Smith, L. M.; Hamers, R. J. *Langmuir* **2002**, *18*, 788.

(15) Strother, T.; Hamers, R. J.; Smith, L. M. *Nucleic Acids Res.* **2000**, *28*, 3535.

(16) Buriak, J. M. *Chem. Rev.* **2002**, *102*, 1271.

(17) Buriak, J. M. *Chem. Commun.* **1999**, 1051.

(18) Stewart, M. P.; Buriak, J. M. *Angew. Chem., Int. Ed.* **1998**, *37*, 3257.

(19) Strother, T.; Knickerbocker, T.; Russell, J. N.; Butler, J. E.; Smith, L. M.; Hamers, R. J. *Langmuir* **2002**, *18*, 968.

(20) Yang, W.; Butler, J. E.; Russell, J. N., Jr.; Hamers, R. J. *Langmuir* **2004**, *20*, 6778.

(21) Lu, M. C.; Knickerbocker, T.; Cai, W.; Yang, W.; Hamers, R. J.; Smith, L. M. *Biopolymers* **2004**, *73*, 606.

(22) Yang, W.; Hamers, R. J. *Appl. Phys. Lett.* **2004**, *85*, 3626.

(23) Härtl, A.; Schmich, E.; Garrido, J.; Hernando, J.; Catharino, S. C. R.; Walter, S.; Feulner, P.; Kromka, A.; Steinmüller, D.; Stutzmann, M. *Nat. Mater.* **2004**, *3*, 736−742.

(24) Alehashem, S.; Chambers, F.; Strojek, J. W.; Swain, G. M.; Ramesham, R. *Anal. Chem.* **1995**, *67*, 2812.

(25) Latto, M. N.; Riley, D. J.; May, P. W. *Diamond Relat. Mater.* **2000**, *9*, 1181.

(26) Swain, G. M.; Ramesham, R. *Anal. Chem.* **1993**, *65*, 345.

(27) Granger, M. C.; Witek, M.; Xu, J. S.; Wang, J.; Hupert, M.; Hanks, A.; Koppang, M. D.; Butler, J. E.; Lucazeau, G.; Mermoux, M.; Strojek, J. W.; Swain, G. M. *Anal. Chem.* **2000**, *72*, 3793.

(28) Kondo, T.; Honda, K.; Tryk, D. A.; Fujishima, A. *Electrochim. Acta* **2003**, *48*, 2739.

(29) Hines, M. A. *Annu. Rev. Phys. Chem.* **2003**, *54*, 29.

(30) Nichols, B.; Hamers, R. J. Manuscript in preparation.

(31) Macdonald, J. R.; Kenan, W. R. *Impedance Spectroscopy—Emphasizing Solid Materials and Systems*; J. Wiley: New York, 1987.

(32) Bard, A. J.; Faulkner, L. *Electrochemical Methods: Fundamentals and Applications*, 2nd ed.; J. Wiley: New York, 2001.

(33) Gerischer, H. *Electrochim. Acta* **1990**, *35*, 1677.

(34) Mott, N. F. *Proc. R. Soc. London, A* **1939**, *171*, 27.

(35) Schottky, W. *Z. Phys.* **1939**, *113*, 367.

(36) Natarajan, A.; Oskam, G.; Searson, P. C. *J. Phys. Chem. B* **1998**, *102*, 7793.

(37) Pleskov, Y. V.; Evstefeeva, Y. E.; Krotova, M. D.; Elkin, V. V.; Maxin, V. M.; Mishuk, V. Y.; Varnin, V. P.; Teremetskaya, I. G. *J. Electroanal. Chem.* **1998**, *455*, 139.

(38) Pleskov, Y. V.; Elkin, V. V.; Abaturov, M. A.; Krotova, M. D.; Mishuk, V. Y.; Varnun, V. P.; Teremetskaya, I. G. *J. Electroanal. Chem.* **1996**, *413*, 105.

(39) Pleskov, Y. V.; Evstefeeva, Y. E.; Krotova, M. D.; Mishuk, V. Y.; Laptev, V. A.; Palyanov, Y. N.; Borzdov, Y. M. *J. Electrochem. Soc.* **2002**, *149*, E260.

(40) Souteyrand, E.; Martin, J. R.; Martelet, C. *Sens. Actuators, B* **1994**, *20*, 63.

(41) Williams, O. A.; Whitfield, M. D.; Jackman, R. B.; Foord, J. S.; Butler, J. E.; Nebel, C. E. *Appl. Phys. Lett.* **2001**, *78*, 3460.

(42) Lanza, V. L.; Herrmann, D. B. *J. Polym. Sci.* **1958**, *28*, 622.

(43) Bousse, L.; de Rooij, N. F.; Bergveld, P. *IEEE Trans. Electron Devices* **1983**, *ED-30*, 1263.

(44) Willner, I.; Willner, B. *Trends Biotechnol.* **2001**, *19*, 222.

(45) Kasu, M.; Kobayashi, N. *Appl. Phys. Lett.* **2002**, *80*, 3961.

(46) Pleskov, Y.; Tameev, A.; Varnin, V. P.; Teremetskaya, I. *J. Solid State Electron.* **1998**, *3*, 25.

(47) Lasseter, T. L.; Clare, B. H.; Abbott, N. L.; Hamers, R. J. *J. Am. Chem. Soc.* **2004**, *126*, 10220.